Decorating beads with paramagnetic rings: synthesis of inorganic-organic [10^{14}]rotaxanes as shown by spin counting

Deepak Asthana,[a,b] Dean Thomas,[a] Selena J. Lockyer,[a] Adam Brookfield,[a] Grigore A. Timco,[a] Iñigo J. Vitorica-Yrezabal,[a] George F. S. Whitehead,[a] Eric J. L. McInnes,[a] David Collison,[a] David A. Leigh[a] and Richard E. P. Winpenny[a]*

[a] *Department of Chemistry, The University of Manchester, Oxford Road, Manchester M13 9Pl, United Kingdom*
[b] *Department of Chemistry, Ashoka University, Sonipat, Haryana, India.*
**Correspondence: richard.winpenny@manchester.ac.uk*

Polymer beads have been used as the core of magnetic particles for around twenty years. Here we report studies to attach polymetallic complexes to polymer beads for the first time, producing beads of around 115 microns that are attached to 10^{14} hybrid inorganic-organic [2]rotaxanes. The bead is then formally a [10^{14}] rotaxane. The number of complexes attached is counted by including TEMPO radicals within the thread of the hybrid [2]rotaxanes, and then performing spin-counting using EPR spectroscopy.

Since 1999 polymer beads have been used as the core of magnetic particles, with Caruso *et al* showing that magnetite could be grown on the exterior of polystyrene.[1] This hugely influential work involved use of a polyelectrolyte attached to the polystyrene core before attachment of Fe_3O_4 nanoparticles. Similar approaches have been used to make core-shell structures with other inorganic materials. ZnS has been grown around polystyrene as a route to photonic crystals[2] and metal-organic framework shells have been grown as a route to particles that can be used to adsorb pollutants.[3,4]

Beads functionalised with paramagnetic molecules have been used in catalysis[5] and studied as agents for dynamic nuclear polarization (DNP).[6] Further functionality has been introduced by blending these properties on or in polymer hosts, and such magnetic polymer beads have been exploited in many areas including sensing, imaging and separations.[7] Radical-bead functionalisation has been used to probe the macromolecular structures of the beads and their swelling on solvation.[8]

We wondered if it was possible to attach polymetallic compounds to a polystyrene bead, which has not been done previously, to our knowledge. This could then be developed in two distinct directions: the attached compound could be decomposed to give a core-shell particle with great control of the metal shell, and perhaps allow formation of different metal-shells than are accessible from synthesis from simple precursors. Secondly, perhaps decorating a bead with a very large number of highly paramagnetic molecules could lead to a use in DNP or as a contrast agent or even as a ferrofluid. However, before speculating on possible applications we needed to establish that the chemistry itself is possible. This is purpose of this report.

Well established chemistry was chosen. To form the link from the bead to the paramagnetic molecule we use conventional copper-catalysed azide-alkyne cycloaddition (CuAAC) click chemistry.[9] To enable this to work we have to functionalise commercially available polystyrene microspheres with pendant azides (Scheme 1) As the polymetallic unit we use {Cr_7Ni} rings that we have studied over a period of years.[10] Here we use the rings as part of a hybrid inorganic-organic [2]rotaxane[11,12] and then perform the click chemistry at one end of a carefully designed thread. We show the chemistry is sufficiently flexible to allow several different [2]rotaxanes to be clicked onto the bead, including [2]rotaxanes that contain organic radicals in addition to the {Cr_7Ni} rings. This has allowed us to perform an elegant

experiment where we count the spins from the organic radicals and that allows us to calculate that 10^{14} rotaxanes are attached to the bead.

We note that the first reported rotaxane was prepared by repetitive statistical threading-and-capping of a polymer-supported macrocycle.[13]

Results

Synthesis

The approach is summarised in Scheme 1 and is based on the {Cr_7Ni} rings form around a secondary ammonium cation template, while the exterior of the ring is covered by sixteen pivalate groups, giving [$(R_2NH_2)Cr_7NiF_8(^tBuCO_2)_{16}$]. Full details are given in the Experimental Procedures Section and the Supplemental Information (Tables S9–12).

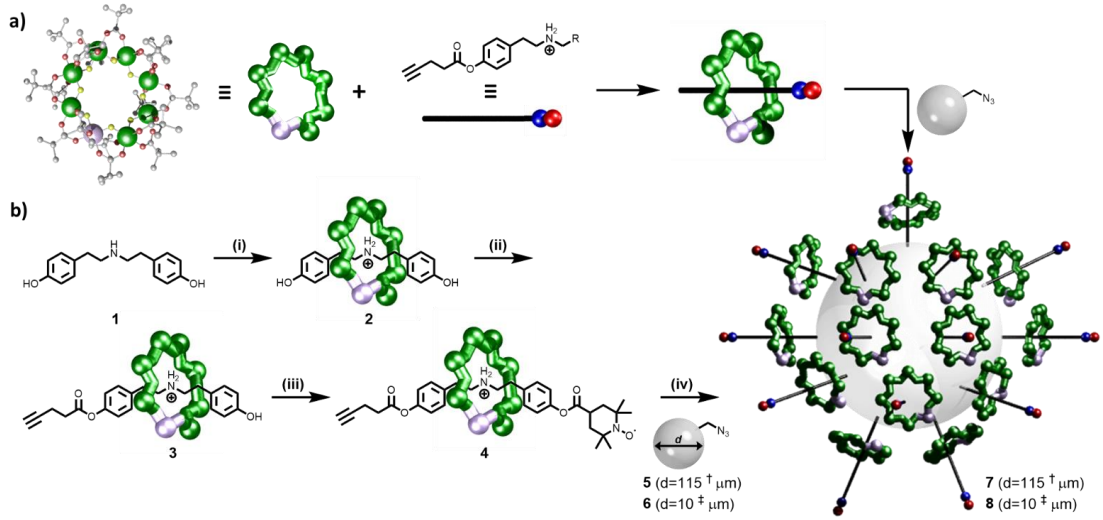

Scheme 1. Synthesis of a decorated bead. a) General overview. b) Reaction conditions: (i) Pivalic acid, $2NiCO_3{\cdot}3Ni(OH)_2{\cdot}4H_2O$, $CrF_3{\cdot}4H_2O$, 140 °C, 24 h; (ii) Pentynoic acid, DCC, DMAP, THF, 50 °C, 16 h; (iii) 4-Carboxy-TEMPO, DCC, DMAP, CH_2Cl_2, RT, 48 h. (iv) Azide-terminated polystyrene beads, $[Cu(MeCN)_4]PF_6$, CH_2Cl_2:DMF (3:2), RT, 72 h. † - 115 ± 35 μm. ‡ - 10 ± 1 μm.

Firstly, the thread $(HOC_6H_4CH_2CH_2)_2NH$ **1** is formed by attaching a terminal phenolic group to an ammonium template. Choice of the distance between the ammonium and phenol unit is important. If the distance is too short, the phenol will be

too sterically hindered for further functionalisation. If the distance is too long, the phenol is esterified by reaction with the pivalic acid used during the formation of the ring.[12] Here, we aimed for an intermediate distance, but a small amount of esterified product is always obtained when **1** is used to form [2]rotaxanes. This ability to control the reactivity of the phenol is important as it allows difunctionalisation of the thread.

Rotaxane **2** was prepared following be reacting **1** with hydrated chromium(III) fluoride and basic nickel carbonate in pivalic acid (See Methods section for preparative details) and was purified by column chromatography. Single crystal X-ray quality crystals of **2** were grown from acetone by slow evaporation. The crystal structure of **2** shows the inorganic-organic [2]rotaxane with the axle terminated by phenols.

To introduce a terminal alkyne for CuAAC click chemistry, rotaxane **2** was reacted with 4-pentynoic acid under Steglich esterification conditions to yield **3**. A second esterification reaction with 4-carboxy-TEMPO gave **4**. Formation of rotaxane **4** was confirmed by electrospray mass spectrometry (ESI-MS), elemental analysis and single crystal X-ray crystallography.

Rotaxane **4** was reacted with azide-functionalised polymer beads **5** or **6** (Scheme 1, see Methods section for preparative details) in a heterogeneous click reaction. After reaction with the rotaxanes, the initially colourless beads turned deep green giving the decorated beads **7** and **8**. To remove any unreacted [2]rotaxane and the catalyst, the beads were then washed repeatedly with CH_3CN, CH_3OH and CH_2Cl_2 following recommended methods.[14]

Product formation was monitored by FT-IR spectroscopy. The IR absorption peak for an azide group around 2090 cm^{-1} was used as a reference. After reaction with [2]rotaxane **4**, a significant decrease in the intensity of the azide band was observed (See SI, section 4). We attribute the small, residual azide band in the IR spectrum to

azide functionalities present in inner, inaccessible regions of the bead.[15] Assuming that all azide sites within 0.5 μm of the surface react, the number of rotaxanes on a single bead of **5** was estimated to be at least 2×10^{13}. For the smaller beads, **6**, we estimate *ca*. 8×10^{10} rotaxanes could be attached (See SI, section 2).

X-ray Crystal Structures

Both **2** and **4** crystallise in monoclinic space groups: $P2_1/c$ and $C2/c$ respectively. The structures are shown in Figure 1. In both structures the eight metals are arranged in an octagon, and the single divalent metal site is not identified by the crystallography, but is disordered about the octagon. Each metal…metal edge is bridged by two carboxylates outside the ring, and by a single fluoride which lies within a cavity. The eight fluorides therefore provide hydrogen bond acceptor sites, and these form H-bonds to the protonated nitrogen of the threads. The metal sites are all six-coordinate, bound to four O- and two F-donors. The metal-ligand distances are very similar to those found in previous $\{Cr_7Ni\}$ rings.[10] For attachment to a bead the key metric is the distance from the terminal C-atom of the alkyne to the N-atom at the ring centre is around 1.36 nm, which allows the CuAAC click reaction to proceed.

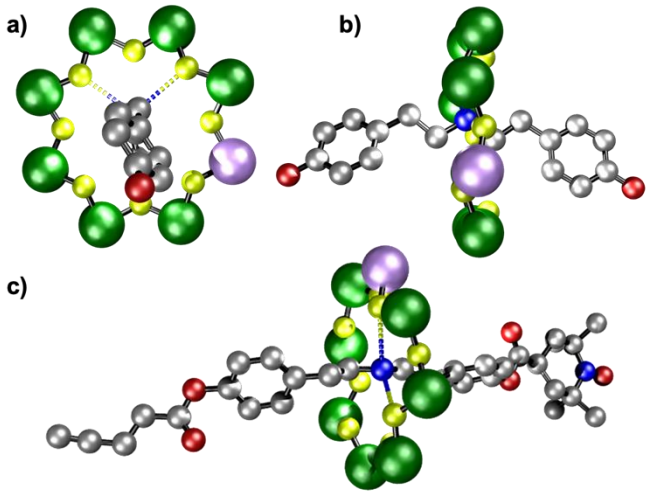

Figure 1. X-Ray crystal structures of **2** and **4**. a) Front and b) side view of **2**. c) Side view of **4** showing terminal alkyne and TEMPO groups. Colours: Cr-green, Ni-aqua, F-yellow, O-red, N-blue and C-grey. Pivalate groups on rings excluded for clarity.

EPR Spectroscopy and spin counting

Continuous wave (CW) Q-Band (ca. 34 GHz) EPR spectra of **4** and **7** were recorded at 5 K. There is a resonance at g = 1.78, which is only observed at low temperature which arises from the S = ½ ground state of the {Cr_7Ni} ring (Figures 2 and S7).[16] This signal is not perturbed between the rotaxane **4** and bead **7**. All spectra were simulated using parameters given in Table 1.

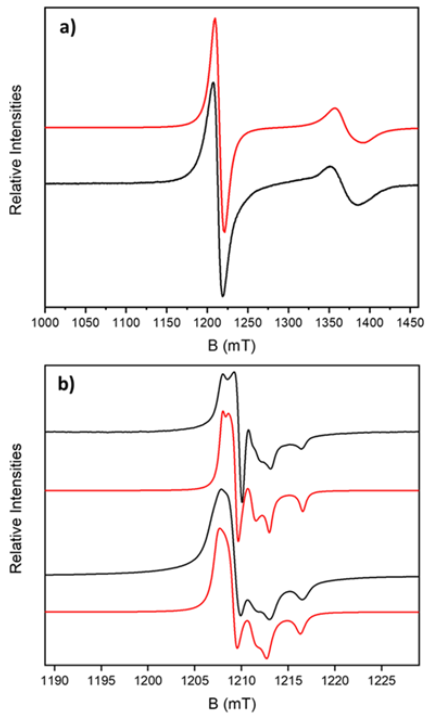

Figure 2: CW Q-Band (ca. 34 GHz) EPR spectra. a) powder sample of **4** at 5 K (black) and simulation (red), with the nitroxide and {Cr_7Ni} resonances. b) Multiple bead samples of **7** at 280 K (black top) and 5K (black bottom), with their respective simulations (red), focused at the nitroxide signal. The experimental frequencies are a) 34.032921 GHz and b) 34.033889 GHz (280 K) and 34.040610 GHz (5 K).

Table 1. EPR simulation parameters for compounds **4**, **7** and **8**						
	T/ K	$NO^{\cdot}$ g values	$^{N}A_z$ /MHz	Line width $NO^{\cdot}$/mT	$\{Cr_7Ni\}$ g values	Line width $\{Cr_7Ni\}$/ mT
4	5	2.0106, 2.0060, 2.0030	100	10	1.788, 1.788, 1.748	20
7	5	2.0106, 2.0060, 2.0030	100	1.2	1.775, 1.775, 1.737	1.2
7	280	2.0097, 2.0057, 2.0026	100	0.8	N/A	N/A
8	5	2.0106, 2.0060, 2.0030	100	5	1.775, 1.775, 1.737	15

Rotaxane **4** and beads **7** and **8** contain TEMPO radicals terminating the thread, and the EPR spectra show resonances for the nitroxides that are observed at all temperatures (Figure 2). In powdered [2]rotaxane **4**, the nitroxide spectrum is broad due to intermolecular interactions, whilst for bead **7** the signal is sharp consistent with dilution of the rings on the bead surface.

The nitroxide signal at RT for **7** makes it possible to quantify the number of nitroxides, and hence the number of threaded rings, on an individual bead, although the values approach the limit of EPR sensitivity.[17] Performing the calculation at lower temperatures is far more demanding, especially due to fluctuations in temperature that could influence the intensity of the signal. It is far easier to perform this at the nitroxide resonance than at the $\{Cr_7Ni\}$ resonance as the nitroxide resonance is visible at room temperature (Figure 2b) and is far sharper than the broad resonance due to the heterometallic ring.

EPR signal intensity calibration curves were constructed from measurements on the [2]rotaxane **4** in toluene solution at room temperature (Figure 3a, see SI, section 5), using twelve concentrations between 0.005 and 0.20 mM (Figures S10 and S11). However, in repeated calibrations we found a discontinuity in the signal intensity as a function of concentration at around 0.07 mM, hence we have restricted spin counting on the beads to calibrant concentrations between 0.005 and 0.06 mM.

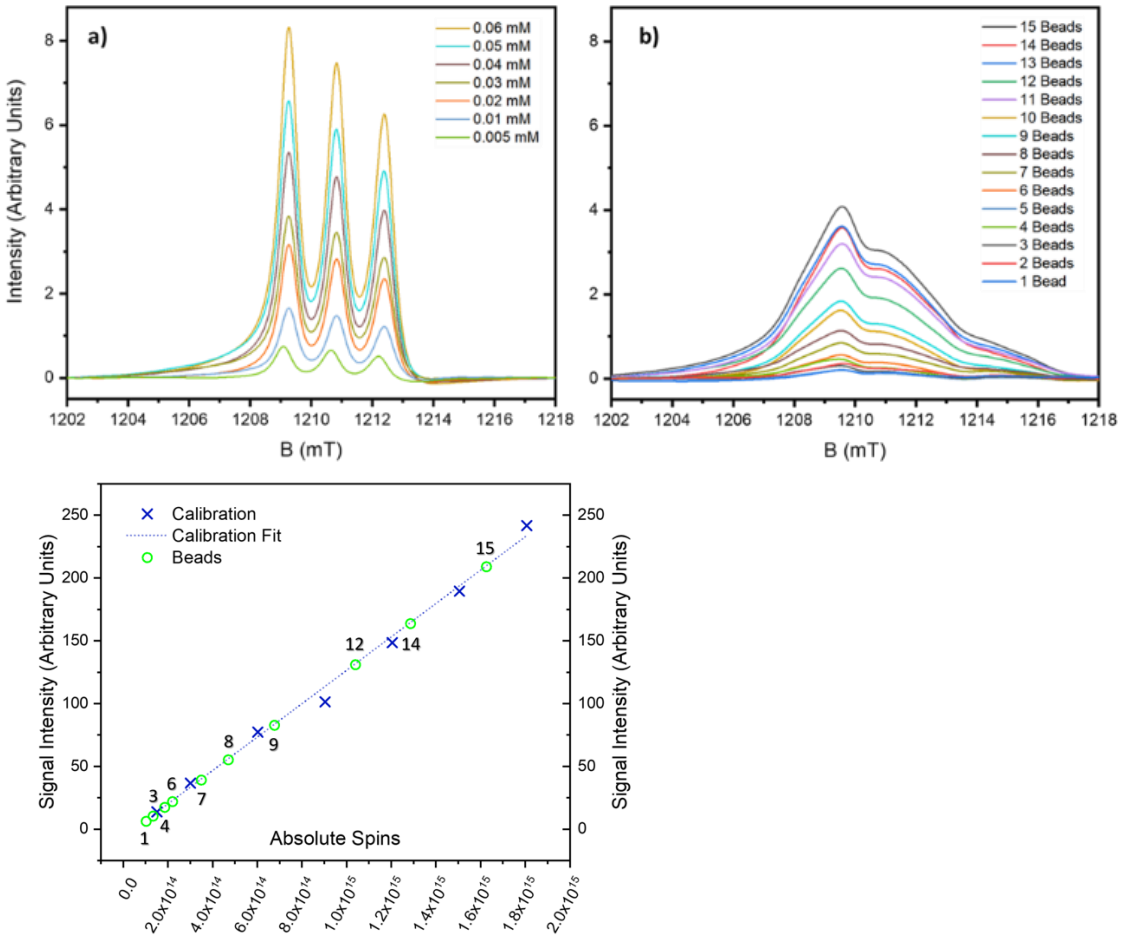

Figure 3: Spin-counting on decorated beads. All spectra recorded at Q-band at room temperature. (a) First integral of Q-band EPR calibration solutions of **4** in toluene. (b) First integral of Q-band EPR spectra varying number of beads of **7**. (c) Spin counting on different numbers of beads **7**, calibrated against a solution of [2]rotaxane **4**. Black figures indicate the number of beads. Measurements for 2, 5, 10, 11 and 13 beads were omitted due to difficulties in obtaining accurate baseline corrections.

Spin counting measurements were then performed on beads of **7** (Figure 3b), using increasing numbers of individual beads from one to fifteen (see SI, section 5 for full details). The signal intensities for the different numbers of beads are mapped onto the calibration curve in Figure 3c.

The number of nitroxide spins per bead was found to be of the order 10^{14} (Table 2). Although the signal intensity increases with number of beads, it does not do so linearly. The detection limit of EPR at these frequencies, temperatures and microwave powers is ca. 10^{12} spins/mT linewidth.[16] Hence, at the lower end of our concentration scale the accuracy of the spin counting experiment is very limited. Moreover, (i) with a single (or a few) beads, positioning of the sample in the EPR tube becomes more crucial, and (ii) there is a distribution of bead sizes with bead diameters between 80-150 μm. Hence, we consider the average number of nitroxide spins per bead from the larger numbers of beads to be the most meaningful. The conclusion is that there are approximately 10^{14} spins per bead, which is within an order of magnitude of the estimated number of rotaxanes (*ca*. 2×10^{13}) from the number of reactive azides (see above).

Table 2. Spin counting of the TEMPO radical signal in **5** measured at 34 GHz and room temperature.

No of beads	Total no. of spins/10^{14}	No of spins per bead/10^{14}
6	2.2	0.4
7	3.5	0.5
8	4.7	0.6
9	6.8	0.8
12	10.4	0.9
14	12.9	0.9
15	16.3	1.1

10 μm diameter beads **6** were also decorated with **4** giving **8**, and these beads were also studied (Figure S8). The mass of the beads measured (1.35 mg) equates to approximately 7.1 × 10^5 beads. The signal intensity observed was compared with our calibration and this leads to 7.2 x 10^{10} spins/bead, which is within an order of magnitude of the estimated number of rotaxanes (*ca*. 8 x 10^{10}). The nitroxide resonance in **4** and **8** is slightly broader than in **7**.

Magnetic measurements

Measuring the magnetic properties of samples containing polystyrene beads presents significant challenges, particularly as there is considerable static between the beads within samples. Nonetheless we have attempted to measure the magnetic properties of two polymer samples: **7** and a bead decorated with [2]rotaxane **10** [$(C_{26}H_{28}NO_4)Cr_7NiF_8(C_5H_7O_2)_{16}$], forming **11** (See Methods section for preparative details) that does not contain the nitroxide radical on the thread. The results are shown in Figure 4.

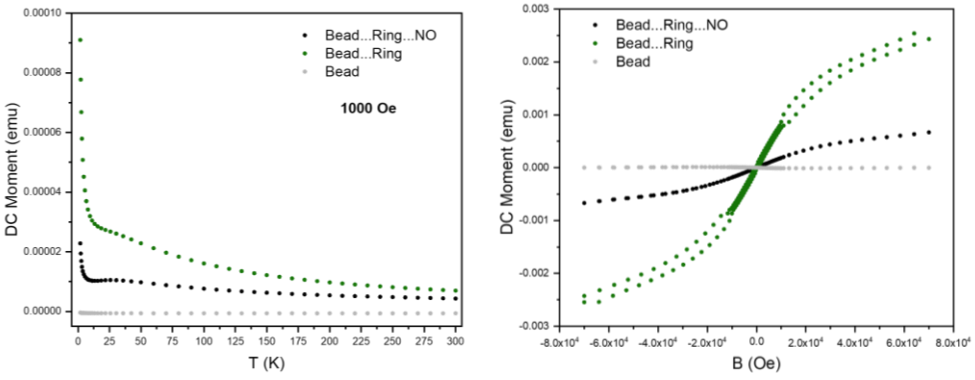

Figure 4. **Magnetic properties of decorated beads**. (a) Variable temperature susceptibility (χ) at 1000 Oe for polymer beads **5** (grey), **7** (green) and **11** (black) normalised to 1 mg of sample. (b) Variable field magnetisation (*M*) at 2 K for polymer beads **5** (grey), **7** (green) and **11** (black) normalised to 1 mg of sample.

At room temperature the susceptibility of **7** and **11** are similar, especially given the limitations of the experiment, and higher than that of the beads alone. As the temperature is lowered the behaviour diverges (Figure 4a). Both show a maximum at around 28 K in $\chi(T)$, which is found in pure samples of the $\{Cr_7Ni\}$ rings.[10] This indicates that the predominant paramagnetic species present are intact $\{Cr_7Ni\}$ rings. However the absolute values of χ diverge considerable. This is even more clear in $M(H)$ at 2 K (Figure 4b). Given the similar values for χ at room temperature this suggests an anti-ferromagnetic interaction between species within **7** that is not present in **11**. Our best explanation at this point is that the additional interaction is between beads, and caused by the longer thread terminated by a radical in **7**, which leads to inter-bead interactions that lower the magnetic response. Another, less paltable, explanation would be that some of the $\{Cr_7Ni\}$ rings have been lost from the rotaxanes in **7**; this would not explain the similar room temperature value for χ in the different samples.

We calculated the magnetic susceptibility for one mg of **11** based on 830 beads per mg. Our calculation for the susceptibility at 300 K, based on the number of rings per bead (10^{14}) and the spins and g-values of Cr^{III} and Ni^{II} (3/2, 1.96 and 1, 2.2 respectively) gave us 7.7 x 10^{-9} emu bead^{-1}, which converts to 6 x 10^{-9} emu mg^{-1}. The measured susceptibility at 300 K is 5 x 10^{-9} emu mg^{-1}, which is surprisingly close.

Conclusions

Microparticles such as **7** and **8** are highly paramagnetic and have been assembled in a very different way to traditional paramagnetic nanoparticles. This demonstrates that CuAAC click chemistry could be generally useful for making highly unusual nanostructures containing hybrid inorganic-organic molecules and supramolecules. In the future we will examine whether such nanoparticles could be used in applications such as DNP.[6]

Acknowledgements

This work was supported by the EPSRC (EP/R043701/1/) including an Established Career Fellowship (EP/R011079/1) to REPW. REPW also thanks the European Research Council for an Advanced Grant (ERC-2017-ADG-786734). DAL thanks the Engineering and Physical Sciences Research Council (EP/P027067/1) and the European Research Council (Advanced Grant No. 786630) for funding. We also thank the EPSRC for an X-ray diffractometer (EP/K039547/1), and for access to the EPR National Facility (NS/A000055/1). We thank the University of Manchester for a President's Scholarship (to DT).

Author Contributions

DA and DT performed the synthetic chemistry, with advice from GAT. SJL measured the EPR spectra, advised by DC and EJLMcI. SJL also solved and refined the X-ray structures, with more challenging refinements completed by IJV-Y and GFSW. DAL and REPW devised the project. The manuscript was written by DA, DT, SJL and REPW with input from all authors.

Competing Interests

The authors declare no competing interests.

Methods

Materials

All chemicals were of reagent grade quality, and they were purchased from commercial sources and used as received. The azide functionalized polystyrene beads were prepared by literature procedures[18,19] (See SI section 1.2). Full characterization details of all compounds are given in the Supplemental Information.

Physical Techniques

^{1}H NMR spectra were recorded on a Bruker AVIII HD 400 MHz at 298 K. Chemical shifts are reported in parts per million (ppm) from high to low frequency using the residual solvent peak as the internal reference (DMSO-d_6 = 2.50 ppm). All ^{1}H resonances are reported to the nearest 0.01 ppm. Infrared spectra were recorded neat on a Bruker FT-IR Alpha II Platinum ATR spectrometer. Fully characterized compounds were chromatographically homogeneous. Flash column chromatography was carried out using Silica 60 Å (particle size 40-63 μm, Sigma Aldrich, UK) as the stationary phase. Analytical TLC was performed on precoated silica gel plates (0.25 mm thick, 60 F254, Merck, Germany) and visualized using both short and longwave ultraviolet light in combination with standard laboratory stains (acidic potassium permanganate, acidic ammonium molybdate and ninhydrin). Low-resolution ESI mass spectrometry and high-resolution mass spectrometry was carried out by staff at the Mass Spectrometry Service, Department of Chemistry, The University of Manchester. Elemental analysis was carried out by the Analytical Service of the University of Manchester; metals analysis by Thermo iCap 6300 inductively coupled plasma optical emission spectroscopy (ICP-OES).

Synthesis of Thread 1

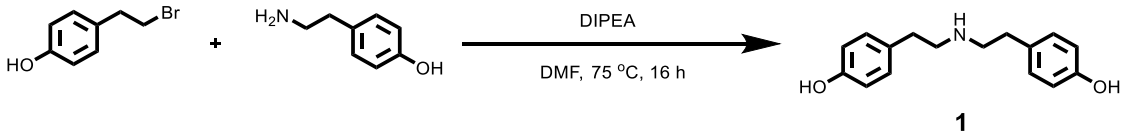

1

To a solution of 2-(4-hydroxyphenyl)-1-bromoethane (2.0 g, 10 mmol) in anhydrous DMF (45 mL) was added 2-(4-hydroxyphenyl)ethylamine (6.0 g, 44 mmol, 4.4 eq.) and *N*-ethyldiisopropylamine (5.2 ml, 30 mmol, 3 eq.). The reaction mixture was heated at 75 °C for 16 hours. When the reaction was complete, the mixture was cooled to room temperature, diluted with EtOAc and washed with brine. The organic phase was dried ($MgSO_4$), filtered, and the solvent removed under reduced pressure. The solid residue was dissolved in hot CH_3OH (100 mL) and precipitated by addition of water (20 mL). The product was filtered and washed repeatedly with $CHCl_3$ to yield the title compound as brown solid (1.8 g, 7.0 mmol, 70%).

Synthesis of Rotaxane 2

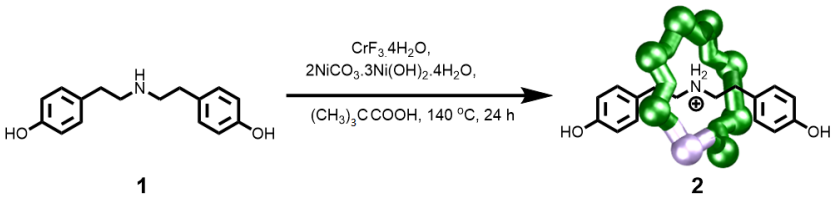

1 **2**

To pivalic acid (45.0 g, 440 mmol) at 100 °C in a Teflon™ flask was added **1** (2.5 g, 9.7 mmol). The reaction mixture was stirred at 100 °C for 10 minutes then [$CrF_3 \cdot 4H_2O$] (6.0 g, 33 mmol) and [$2NiCO_3 \cdot 3Ni(OH)_2 \cdot 4H_2O$] (1.0 g, 1.7 mmol) were added. The reaction mixture was stirred at 140 °C for 24 hours. The reaction mixture was cooled to room temperature and the crude product was extracted with $CHCl_3$. The solvent was removed under reduced pressure and the crude residue was purified by column

chromatography (SiO_2, $CHCl_3$:EtOAc, 90:10) to yield rotaxane **2** (3.5 g, 1.4 mmol, 15%).

Synthesis of Rotaxane 4

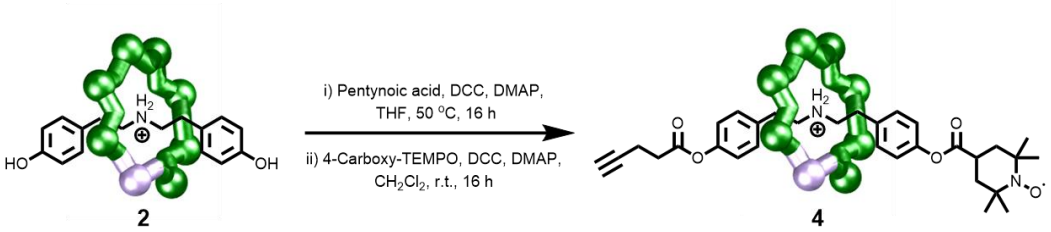

To prepare molecule **4**, a two-step esterification was performed. Firstly, to a solution of rotaxane **2** (3.0 g, 1.2 mmol), in THF (100 ml) was added pentynoic acid (0.12 g, 1.2 mmol), DCC (0.90 g, 4.3 mmol) and DMAP (0.75 g, 6.1 mmol). The reaction mixture was stirred at 50 °C for 16 hours. The solvent was removed under reduced pressure and the crude residue was purified by column chromatography (SiO_2, $CHCl_3$:EtOAc, 95:5) to yield mono-esterified rotaxane **3** (0.75 g, 0.30 mmol, 25%).

To a solution of rotaxane **3** (0.75 g, 0.30 mmol) in CH_2Cl_2 (50 mL) was added 4-carboxy-TEMPO (0.18 g, 0.90 mmol), DCC (0.55 g, 2.6 mmol) and DMAP (0.55 g, 4.5 mmol). The reaction mixture was stirred at room temperature for 16 hours. The solvent was removed under reduced pressure and the crude residue was purified by column chromatography (SiO_2, $CHCl_3$:CH_3OH, 95:5) to yield rotaxane **4** (0.65 g, 0.24 mmol, 80%).

Synthesis of Bead-Rotaxane 7

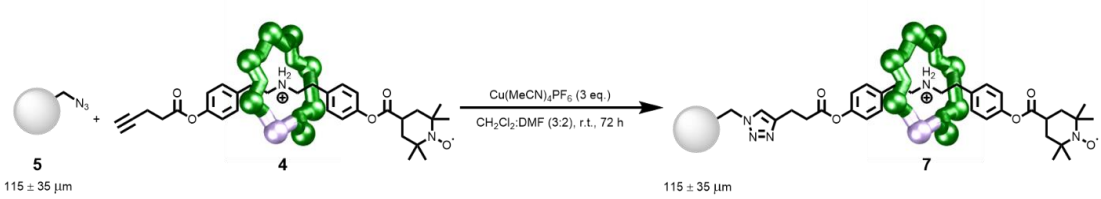

Azide polystyrene beads **5** (3.0 mg, 1.3 mmol g^{-1}, 3.9 µmol) were added to $[(C_{31}H_{40}N_2O_5)Cr_7NiF_8(C_5H_9O_2)_{16}]$ **4** (30 mg, 11 µmol, 3 eq.) and $Cu(MeCN)_4PF_6$ (4.0 mg, 11 µmol, 3 eq.) under argon. A CH_2Cl_2:DMF mixture (3:2, 5 mL, degassed with argon) was added and the reaction was stirred for 72 hours at room temperature. The reaction mixture was then filtered and washed with CH_3CN (3 × 10 mL), CH_3OH (3 × 10 mL), and CH_2Cl_2 (3 × 10 mL) to afford [2]rotaxane–polystyrene beads **7** (13.0 mg, 3.7 µmol).

Synthesis of Bead-Rotaxane 8

Azide polystyrene beads **6** (2.5 mg, 1.0 mmol g^{-1}, 2.5 μmol) were added to $[(C_{31}H_{40}N_2O_5)Cr_7NiF_8(C_5H_9O_2)_{16}]$ **4** (30 mg, 11 μmol, 4 eq.) and $Cu(MeCN)_4PF_6$ (5.0 mg, 13 μmol, 5 eq.) under argon. A CH_2Cl_2:DMF mixture (3:2, 5 mL, degassed with argon) was added and the reaction was stirred for 72 hours at room temperature. The reaction mixture was then filtered and washed with CH_3CN (3 × 10 mL), CH_3OH (3 × 10 mL), and CH_2Cl_2 (3 × 10 mL) to afford [2]rotaxane–polystyrene beads **8** (8.3 mg, 2.4 μmol).

Synthesis of Rotaxane 10

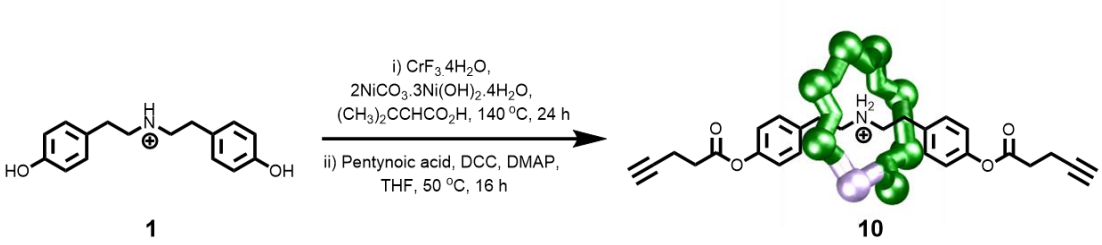

To 3,3-dimethylacrylic acid (15.0 g, 150 mmol) in a Teflon™ flask was added **1** (1.5 g, 5.8 mmol) and 5.0 ml of 1,2-dichlorobenzene and heated to 140 °C for 10 minutes. To this solution $[CrF_3 \cdot 4H_2O]$ (3.0 g, 16 mmol) and $[2NiCO_3 \cdot 3Ni(OH)_2 \cdot 4H_2O]$ (0.75 g, 1.2 mmol) were added and stirred at 140 °C for 24 hours. The reaction mixture was cooled to room temperature, transferred in to a 500 ml flask and 300 ml of hexane was added. The crude product was extracted with diethyl ether and purified by column

chromatography (Silica, toluene/EtOAc) to yield rotaxane **9** (2.5 g). Single crystal X-ray quality crystals were grown from acetone by slow evaporation method.

To prepare rotaxane **10**, to a solution of rotaxane **9** (2.0 g, 0.8 mmol), in THF (100 ml) was added pentynoic acid (0.2 g, 2.0 mmol), DCC (0.3 g, 1.4 mmol) and DMAP (0.25 g, 2.0 mmol). The reaction mixture was stirred at 50 °C for 16 hours. The solvent was removed under reduced pressure and the crude residue was purified by column chromatography (SiO_2, $CHCl_3$:EtOAc, 95:5) to yield **10**. Single crystal X-ray quality crystals were grown from acetone by slow evaporation method.

Synthesis of Bead-Rotaxane 11

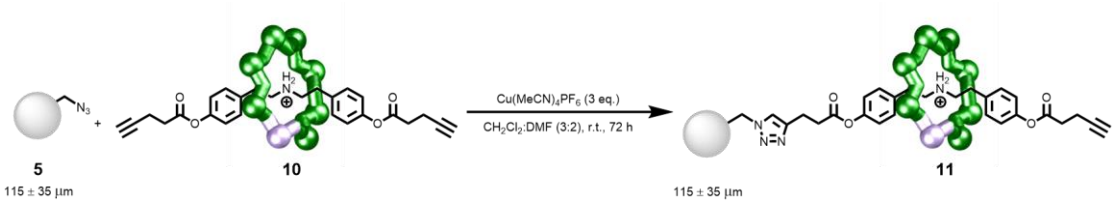

Azide polystyrene beads **5** (7.0 mg, 1.3 mmol g^{-1}, 9.0 µmol) were added to $[(C_{26}H_{28}NO_4)Cr_7NiF_8(C_5H_7O_2)_{16}]$ **10** (72 mg, 27 µmol, 3 eq.) and $Cu(MeCN)_4PF_6$ (10 mg, 27 µmol, 3 eq.) under argon. A CH_2Cl_2:DMF mixture (3:2, 5 mL, degassed with argon) was added and the reaction was stirred for 72 hours at room temperature. The reaction mixture was then filtered and washed with CH_3CN (3 × 10 mL), CH_3OH (3 × 10 mL), and CH_2Cl_2 (3 × 10 mL) to afford [2]rotaxane–polystyrene beads **11** (28 mg, 8.8 µmol).

Single-Crystal X-ray Diffraction

X-Ray data for compounds **2**, **4**, and **9** were collected at a temperature of 100 K using a dual wavelengh Rigaku FR-X with Cu-Kα radiation equipped with a HypixHE6000 detector and an Oxford Cryosystems nitrogen flow gas system. X-ray data for compound **10** was collected at a temperature of 100 K using synchrotron radiation at beamline I19 in Diamond Light Source equipped with a Pilatus 2M detector and an Oxford Cryosystems nitrogen flow gas system. Data was measured using GDA and CrysAlisPro suite of programs.

X-Ray data were processed and reduced using CrysAlisPro suite of programmes. Absorption correction was performed using empirical methods (SCALE3 ABSPACK) based upon symmetry-equivalent reflections combined with measurements at different azimuthal angles.[20] The crystal structure was solved and refined against all F^2 values using the SHELXL[21] and Olex 2 suite of programmes.[22]

All atoms in crystal structures were refined anisotropically with the exception of the hydrogen atoms, that were placed in the calculated idealized positions for all crystal structures. The pivalate ligands, and threads in crystal structures were disordered and modelled over two positions, using structural same distance (SADI) and distance fix (DFIX) Shelxl restraints commands. The atomic displacement parameters (adp) of the ligands have been restrained using similar Ueq and rigid bond (SIMU) and Similar Ueq (SIMU) restraints.

Spectroscopic Measurements.

Q-band (*ca.* 34 GHz) EPR spectra were recorded with a Bruker EMX580 spectrometer at the EPRSC National UK EPR Facility and Service at The University of Manchester. The data were collected on polycrystalline powders and on solid polymeric beads at

280 K, and 5 K using liquid helium cooling. Spectral simulations were performed using the *EasySpin 4.5.5* simulation software.[23]

Magnetic measurements

Magnetic properties were measured on a Quantum Design MPMS3. Susceptibility was measured from 300 to 2 K in a 1000 Oe magnetic field. Magnetisation was measured at 2 K to a maximum field of 7 T. Samples were mounted in gelatine capsules. The mass of samples measured were: **5,** 21.83 mg; **7**, 7.04 mg; **11**, 14.28 mg. No diamagnetic correction has been applied to data. For **11** beads were counted and weighed and this leads to an estimate of 831 beads per mg which we have used in calculations.

Data availability

Supplementary information is available in the online version of the paper. CCDC 2058841, 2058842, 2058844 and 2058846 numbers contain the supplementary crystallographic data for this paper. These data can be obtained free of charge *via* www.ccdc.cam.ac.uk/conts/retrieving.html (or from the Cambridge Crystallographic Data Centre, 12 Union Road, Cambridge CB21EZ, UK; fax: (+44)1223-336-033; or deposit@ccdc.cam.ac.uk). Reprints and permissions information is available online at www.nature.com/reprints. Correspondence and requests for materials should be addressed to R. E. P. W.

References

1. Caruso, F. Susha, A. S., Giersig, M. & Möhwald, H. Magnetic core-shell particles: preparation of magnetite multilayers on polymer latex microspheres. *Adv. Mater.* **11**, 950–953 (1999).

2. Breen, M. L., Dinsmore, A. D., Pink, R. H., Qadri, S. B. & Ratna, B. R. Sonochemically produced ZnS-coated polystyrene core-shell particles for use in photonic crystals. *Langmuir* **17**, 903–907 (2001).

3. Del Rio, M., Cabello, C. P., Gonzalez, V., Maya, F., Parra, J. B., Cerdà, V. & Palomino, G. T. Metal oxide assisted preparation of core-shell beads with dense metal-organic framework coatings for the enhanced extraction of organic pollutants. *Chem. Eur. J.* **22**, 11770–11777 (2016).

4. Kuo, Y. -C., Pal, S., Li, F. -Y. & Lin, C. -H. Polystyrene-supported core-shell beads with aluminium MOF coating for extraction of organic pollutants. *Chem. Asian J.* **14**, 3675–3681 (2019).

5. Bukowska, A., Bester, K., Pytel, M. & Bukowski, W. Polymer Beads Decorated with Dendritic Systems as Supports for A^3 Coupling Catalysts. *Catal. Lett*. **151**, 422–4434 (2021).

6. Zhang, Y., Baker, P. J. & Casabianca, L. B. BDPA-Doped Polystyrene Beads as Polarization Agents for DNP-NMR. *J. Phys. Chem. B*, **120**, 18–24 (2016).

7. Philipova, O., Barabanova, A., Molchanov, V. & Khokhlov, A. Magnetic polymer beads: Recent trends and developments in synthetic design and applications. *Eur. Polymer J*., **47**, 542–559 (2011).

8. Marchetto, R., Cilli, E. M., Jubuilut, G. N., Schreier, S. & Nakaie, C. R. Determination of Site−Site Distance and Site Concentration within Polymer

Beads: A Combined Swelling-Electron Paramagnetic Resonance Study. *J. Org. Chem*., **70**, 4561–4568 (2005).

9. Liang, L. & Astruc, D. The copper(I)-catalyzed alkyne-azide cycloaddition (CuAAC) "click" reaction and its applications. An overview. *Coord. Chem. Rev*. **255**, 2933–2945 (2011).

10. McInnes, E. J. L., Whitehead, G. F. S., Timco, G. A. & Winpenny, R. E. P. Heterometallic Rings as a Playground for Physics and Supramolecular Building Blocks. *Angew. Chem. Int. Ed.,* **54**, 14244–14269 (2015).

11. Lee, C.- F. *et al.* Hybrid organic-inorganic rotaxanes and molecular shuttles. *Nature* **458**, 314–318 (2009).

12. Ballesteros, B. *et al.* Synthesis, Structure and Dynamic Properties of Hybrid Organic-Inorganic Rotaxanes. *J. Am. Chem. Soc.* **132**, 15435–15444 (2010).

13. Harrison, I. T. & Harrison, S. Synthesis of a stable complex of a macrocycle and a threaded chain. *J. Am. Chem. Soc*. **89**, 5723–5724 (1967).

14. Townsend, J. B., Shaheen, F., Liu R. & Lam, K. S. Jeffamine Derivatized TentaGel Beads and Poly(dimethylsiloxane) Microbead Cassettes for Ultrahigh-Throughput in Situ Releasable Solution-Phase Cell-Based Screening of One-Bead-One-Compound Combinatorial Small Molecule Libraries. *J. Comb. Chem.*, **12**, 700–712 (2010).

15. Sherrington, D. C. Preparation, structure and morphology of polymer supports. *Chem. Commun*. **21**, 2275–2286 (1998).

16. Piligkos, S., Weihe, H., Bill, E., Neese, F., El Mkami, H., Smith, G. M., Collison, D., Rajaraman, G., Timco, G. A., Winpenny, R. E. P. & McInnes, E. J. L. EPR Spectroscopy of a Family of $Cr^{III}7M^{II}$ (M = Cd, Zn, Mn, Ni)

"Wheels": Studies of Isostructural Compounds with Different Spin Ground States. *Chem. Eur. J.* **15**, 3152–3167 (2009).

17. Möser, J. *et al.* Using rapid-scan EPR to improve the detection limit of quantitative EPR by more than one order of magnitude. *J. Magn. Reson.*, 2017, **281**, 17–25 (2017).

18. Bettinetti L., Lober S., Hubner, H. & Gmeiner, P. Parallel Synthesis and Biological Screening of Dopamine Receptor Ligands Taking Advantage of a Click Chemistry Based BAL Linker. *J. Comb. Chem*. **7**, 309–316 (2005).

19. Arseniyadis, S., Wagner, A. & Mioskowski, C. A straightforward preparation of amino–polystyrene resin from Merrifield resin. *Tetrahedron Lett*. **43**, 9717–9719 (2002).

20. Rigaku Oxford Diffraction, CrysAlisPro Software system version 1.171.37.33 (Rigaku Corporation, Oxford, UK, 2018).

21. Sheldrick, G. M. A short history of SHELX. *Acta Crystallogr.* **A71**, 3–8 (2015).

22. Dolomanov, O. V., Bourhis, L. J., Gildea, R. J., Howard, J. A. K. & Puschmann, H. OLEX2: a complete structure solution, refinement and analysis program. *J. Appl. Cryst.* **42**, 339–341 (2009).

23. Stoll, S. & Schweiger, A. EasySpin, a comprehensive software package for spectral simulation and analysis in EPR. *J. Magn. Reson.* **178**, 42-55 (2006).